^{18}F-Fluorobenzoate–Labeled Cystine Knot Peptides for PET Imaging of Integrin $\alpha_v\beta_6$

Benjamin J. Hackel*[1], Richard H. Kimura*[1], Zheng Miao[1], Hongguang Liu[1], Ataya Sathirachinda[1], Zhen Cheng[1], Frederick T. Chin[1], and Sanjiv S. Gambhir[1,2]

[1]*Department of Radiology, Molecular Imaging Program at Stanford, Canary Center for Cancer Early Detection, Stanford University, Stanford, California; and* [2]*Department of Bioengineering, Department of Materials Science and Engineering, Stanford University, Stanford, California*

Integrin $\alpha_v\beta_6$ is a cell surface receptor minimally expressed by healthy tissue but elevated in lung, colon, skin, ovarian, cervical, and pancreatic cancers. A molecular PET agent for integrin $\alpha_v\beta_6$ could provide significant clinical utility by facilitating both cancer staging and treatment monitoring to more rapidly identify an effective therapeutic approach. **Methods:** Here, we evaluated 2 cystine knot peptides, $R_0$1 and $S_0$2, previously engineered with a 3–6 nM affinity for integrin $\alpha_v\beta_6$, for ^{18}F radiolabeling and PET imaging of BxPC3 pancreatic adenocarcinoma xenografts in mice. Cystine knot peptides were labeled with *N*-succinimidyl-4-^{18}F-fluorobenzoate and evaluated for binding affinity and serum stability. Peptides conjugated with ^{18}F-fluorobenzoate (2–3 MBq) were injected via the tail vein into nude mice xenografted with BxPC3 (integrin $\alpha_v\beta_6$–positive) or 293 (integrin $\alpha_v\beta_6$–negative) tumors. Small-animal PET scans were acquired at 0.5, 1, and 2 h after injection. Ex vivo γ-counting of dissected tissues was performed at 0.5 and 2 h. **Results:** ^{18}F-fluorobenzoate peptides were produced in 93% (^{18}F-fluorobenzoate-$R_0$1) and 99% (^{18}F-fluorobenzoate-$S_0$2) purity. ^{18}F-fluorobenzoate-$R_0$1 and ^{18}F-fluorobenzoate-$S_0$2 had affinities of 1.1 ± 0.2 and 0.7 ± 0.4 nM, respectively, and were 87% and 94%, respectively, stable in human serum at 37°C for 2 h. ^{18}F-fluorobenzoate-$R_0$1 and ^{18}F-fluorobenzoate-$S_0$2 exhibited 2.3 ± 0.6 and 1.3 ± 0.4 percentage injected dose per gram (%ID/g), respectively, in BxPC3 xenografted tumors at 0.5 h (n = 4–5). Target specificity was confirmed by low tumor uptake in integrin $\alpha_v\beta_6$–negative 293 tumors (1.4 ± 0.6 and 0.5 ± 0.2 %ID/g, respectively, for ^{18}F-fluorobenzoate-$R_0$1 and ^{18}F-fluorobenzoate-$S_0$2; both $P < 0.05$; n = 3–4) and low muscle uptake (3.1 ± 1.0 and 2.7 ± 0.4 tumor to muscle for ^{18}F-fluorobenzoate-$R_0$1 and ^{18}F-fluorobenzoate-$S_0$2, respectively). Small-animal PET data were corroborated by ex vivo γ-counting of dissected tissues, which demonstrated low uptake in nontarget tissues with only modest kidney uptake (9.2 ± 3.3 and 1.9 ± 1.2 %ID/g, respectively, at 2 h for ^{18}F-fluorobenzoate-$R_0$1 and ^{18}F-fluorobenzoate-$S_0$2; n = 8). Uptake in healthy pancreas was low (0.3% ± 0.1% for ^{18}F-fluorobenzoate-$R_0$1 and 0.03% ± 0.01% for ^{18}F-fluorobenzoate-$S_0$2; n = 8). **Conclusion:** These cystine knot peptide tracers, in particular ^{18}F-fluorobenzoate-$R_0$1, show translational promise for molecular imaging of integrin $\alpha_v\beta_6$ overexpression in pancreatic and other cancers.

Key Words: integrin $\alpha_v\beta_6$; positron emission tomography; cystine knot

J Nucl Med 2013; 54:1101–1105
DOI: 10.2967/jnumed.112.110759

Integrin $\alpha_v\beta_6$ is emerging as a potentially useful molecular marker of multiple cancers. Integrin $\alpha_v\beta_6$ overexpression has been demonstrated in oral squamous cell carcinoma (*1*), pancreatic ductal adenocarcinomas (*2*), intestinal gastric carcinomas (*2*), ovarian cancer (*3*), and stage III basal cell carcinoma (*4*). Moreover, overexpression is prognostic of reduced survival in colon carcinoma (*5*), non–small cell lung cancer (*6*), cervical squamous carcinoma (*7*), and gastric carcinoma (*8*). Also, integrin $\alpha_v\beta_6$ expression is associated with increased liver metastasis of colon cancer (*9*). Importantly, expression is undetectable in most normal tissues including ovary (*3*); kidney, lung, and skin (*1*); and pancreas (*2*). Thus, a molecular imaging agent targeted to integrin $\alpha_v\beta_6$ would provide significant clinical utility.

The linear peptide A20FMDV2, derived from the envelope protein of foot-and-mouth disease, has a concentration of half-maximal inhibition of 3 ± 1 nM for integrin $\alpha_V\beta_6$ (*10*). The ^{18}F-radiolabeled peptide exhibited an uptake of 0.7 ± 0.1 percentage injected dose per gram (%ID/g) of tumor in xenografted mice but only a ratio of 1.2 ± 0.6 tumor to muscle at 1 h. Moreover, this peptide analyzed in the urine at 1 h was fully degraded to multiple metabolites. Polyethylene glycol conjugation of this peptide improved tumor uptake to 1.9 ± 0.4 %ID/g and tumor to muscle to 2.5, though significant metabolic breakdown was still present (*11*). An alternative linear peptide targeted to integrin $\alpha_v\beta_6$, HBP-1, yielded no tumor-to-blood contrast (*12*).

To identify a more stable and effective molecular imaging agent, we have recently engineered cystine knot peptides with a 3–6 nM affinity for integrin $\alpha_v\beta_6$ (*13*). ^{64}Cu labeling of these peptides via a DOTA chelator enabled effective PET imaging of mice bearing BxPC3 pancreatic adenocarcinoma and A431 epidermoid carcinoma xenografted tumors. Tumor uptake with an arginine-rich scaffold was 4.7 ± 0.9 %ID/g at 1 h with 8.7 ± 1.5 tumor-to-muscle contrast, and the peptide was 80% stable in serum for 24 h. A serine-rich cystine knot peptide had 2.1 ± 0.5 %ID/g tumor, 9.4 ± 1.7 tumor to muscle, and greater than 95% serum stability at 24 h. The rapid tumor localization and background clearance of these small peptides enable imaging as early as 1 h after injection. Thus,

Received Jul. 2, 2012; revision accepted Jan. 14, 2013.
For correspondence or reprints contact: Sanjiv S. Gambhir, 318 Campus Dr. MC5427, Stanford, CA 94305.
E-mail: sgambhir@stanford.edu
*Contributed equally to this work.
Published online May 13, 2013.

^{18}F is a preferred radioisotope for clinical translation of these agents because of its greater positron yield and faster decay (for reduced radiation exposure).

In the current work, we evaluate two ^{18}F-labeled integrin $\alpha_v\beta_6$–targeted cystine knot peptides for small-animal PET imaging of pancreatic adenocarcinoma xenografted tumors in mice. Pancreatic cancer is of particular interest because of its rapid lethality (6% five-y survival (*14*)). A molecular imaging tracer for PET would be clinically valuable for both cancer staging and treatment monitoring to more rapidly identify an effective therapeutic approach.

MATERIALS AND METHODS

Peptide Synthesis and Radiochemistry

Peptides $R_0$1 and $S_0$2 were synthesized using standard Fmoc chemistry, folded, and purified by reversed-phase high-performance liquid chromatography (RP-HPLC) as described previously (*13*). Protein mass was verified by matrix-assisted laser desorption/ionization–time-of-flight–mass spectrometry (MALDI-TOF-MS). The amine-reactive radiolabeling agent *N*-succinimidyl-4-^{18}F-fluorobenzoate (^{18}F-SFB) was synthesized using TRACERlab FX-FN (*15,16*). The triflate precursor 4-(ethoxycarbonyl)-*N,N,N*-trimethylbenzenaminium (3 mg) was reacted with the dried ^{18}F-fluoride-Kryptofix-K_2CO_3 complex (6.8 GBq) at 90°C for 10 min (Kryptofix supplier, Sigma Aldrich). ^{18}F-4-fluorobenzoic acid was prepared by reaction with tetrapropylammonium hydroxide (50 μmol) at 120°C for 3 min. Acetonitrile was added and evaporated to remove residual water. The reaction mixture was added to 10 mg of *O*-(*N*-succinimidyl)-1,1,3,3-tetramethyluronium tetrafluoroborate (10 mg) and heated at 90°C for 5 min to produce ^{18}F-SFB. Acetic acid (8 mL; 5% v/v) was added and used to transfer the crude reaction mixture to a dilution flask with 12 mL of water. The mixture was passed through a C18 Plus cartridge (Waters), washed with 10% acetonitrile in water (10 mL), and eluted with acetonitrile (3 mL). ^{18}F-SFB was dried under vacuum at 60°C, resuspended in dimethyl sulfoxide (50 μL), and reacted with folded peptide (~300 μg) in 0.1 M sodium phosphate, pH 7.5 (300 μL), at 50°C for 45 min. ^{18}F-fluorobenzoate-peptide was purified by semipreparative RP-HPLC on a C18 column using a gradient of 25%–65% over 35 min for $R_0$1 and 22.5%–27.5% over 35 min for $S_0$2. Solvent was removed by rotary evaporation, and peptide was prepared in phosphate-buffered saline.

Affinity Titration

$R_0$1 and $S_0$2 were labeled with cold SFB to produce fluorobenzoate-peptide. Yeast surface-display competition assays were performed to measure the binding affinity of fluorobenzoate-peptide as described previously (*17*). EBY100 *Saccharomyces cerevisiae* yeast were transformed with plasmid to encode $R_0$1. Yeast were grown, and $R_0$1 expression was induced. Yeast were washed and incubated with 100 pM to 300 nM fluorobenzoate-peptide and 10 nM soluble integrin $\alpha_v\beta_6$. Yeast were washed and labeled with a fluorescein-conjugated antiintegrin α_v antibody. Fluorescence was quantified by flow cytometry. The concentration of half-maximal inhibition was calculated by minimizing the sum of squared error. The equilibrium dissociation constant was calculated using the Cheng–Prusoff equation (*18*).

Serum Stability

^{18}F-fluorobenzoate-peptide in phosphate-buffered saline was mixed with an equal volume of human serum and incubated at 37°C, 300 rpm, for 2 h. Trifluoroacetic acid was added, and the soluble fraction was clarified with a 0.22-μm filter. The sample was separated by RP-HPLC on a C18 column with a gradient of 5%–85% acetonitrile in water (both with 0.1% trifluoroacetic acid) from 5 to 35 min and analyzed with a γ-ray detector.

Small-Animal Imaging and Tissue Biodistribution

Animal experiments were conducted in accordance with federal and institutional regulations under a protocol approved by the Stanford University Institutional Animal Care and Use Committee. Ten million integrin $\alpha_v\beta_6$–positive BxPC3 pancreatic adenocarcinoma cells or integrin $\alpha_v\beta_6$–negative HEK-293 cells were subcutaneously injected into the shoulder of 6-wk-old female *nu/nu* mice. Xenografted tumors were grown to a 10-mm diameter. Mice were anesthetized with isoflurane and injected via the tail vein with 2–3 MBq of ^{18}F-fluorobenzoate-peptide. A rodent R4 microPET (Siemens) scanner was used to acquire 5-min static scans at 0.5, 1, and 2 h after injection or a 10-min dynamic scan. Tumor, kidney, liver, and hind leg muscle signals were quantified with AsiPro VM (Siemens) for static scans and AMIDE (Amide's a Medical Imaging Data Examiner) (*19*) for dynamic scans. For excised tissue biodistribution, at 0.5 and 2 h after injection mice were euthanized, tissues were collected and weighed, and activity was measured with a γ-ray counter. The decay-corrected activity per mass of tissue was calculated. All data are presented as mean ± SD. Statistical significance was tested using the 2-tailed Student *t* test, with a threshold of *P* less than 0.05. For coinjection studies, 250 μg of unlabeled $R_0$1 or $S_0$2 were coinjected along with the corresponding ^{18}F-fluorobenzoate-peptide. Mice were analyzed for biodistribution in excised tissues.

RESULTS

Peptide Synthesis and Radiochemistry

Peptides $R_0$1 and $S_0$2 (Fig. 1) were synthesized using standard Fmoc chemistry. Mass was verified by MALDI-TOF-MS: $R_0$1, 3,908.7 Da (3,908.8 Da expected); and $S_0$2, 3,875.5 Da (3,874.7 Da expected). Peptides were folded and purified by RP-HPLC. The abstraction of 6 hydrogens during oxidation was verified by MALDI-TOF-MS: $R_0$1, 3,902.8 Da; and $S_0$2, 3,868.4 Da. ^{18}F-SFB was synthesized in 1 h with a 23% ± 13% yield (decay-corrected to start of synthesis). Three hundred micrograms of folded peptide were reacted with approximately 1,000 MBq of ^{18}F-SFB in 0.1 M sodium phosphate, pH 7.5, at 50°C for 45 min. ^{18}F-fluorobenzoate-peptide was purified by RP-HPLC. Solvent was removed by rotary evaporation, and product was resuspended in phosphate-buffered saline. ^{18}F-fluorobenzoate-$R_0$1 and ^{18}F-fluorobenzoate-$S_0$2 were 93% and more than 99% pure as measured by analytic RP-HPLC. Decay-corrected yield from ^{18}F-SFB was 7% ± 1% for ^{18}F-fluorobenzoate-$R_0$1 and 6% ± 1% for ^{18}F-fluorobenzoate-$S_0$2. ^{18}F-fluorobenzoate-$R_0$1 and ^{18}F-fluorobenzoate-$S_0$2 were 87% and 94% stable for 2 h at 37°C in human serum (Fig. 2). In a binding competition assay using 10 nM soluble integrin $\alpha_V\beta_6$, the concentration of half-maximal inhibition values of fluorobenzoate-$R_0$1 and fluo-

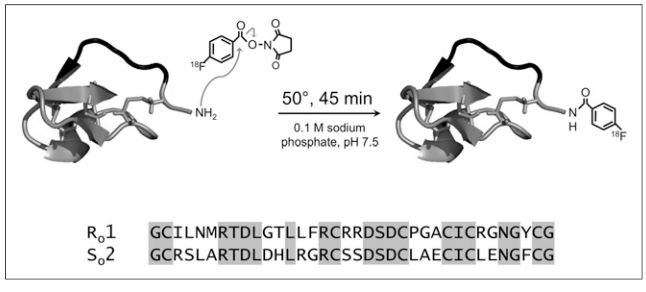

FIGURE 1. Cystine knot peptides. $R_0$1 and $S_0$2 are cystine knot peptides that contain 3 disulfide bonds, an active binding loop (black), and a sole primary amine at N terminus. N-terminal amine was coupled with ^{18}F-SFB in 0.1 M sodium phosphate, pH 7.5, at 50°C for 45 min. Peptide sequences are presented with conserved residues highlighted.

robenzoate-$S_0$2 were measured as 4.1 ± 0.6 and 2.7 ± 1.6 nM, respectively. These correspond to equilibrium dissociation constant values of 1.1 ± 0.2 and 0.7 ± 0.4 nM, respectively (Supplemental Fig. 1; supplemental materials are available online only at http://jnm.snmjournals.org).

Small-Animal PET Imaging

The radiolabeled peptides were used for small-animal PET imaging of mice bearing BxPC3 pancreatic adenocarcinoma xenografted tumors. Nude mice were inoculated with 10^7 BxPC3 cells, which express integrin $\alpha_v\beta_6$. When tumors reached approximately 10 mm in diameter, mice were injected with 2–3 MBq of ^{18}F-fluorobenzoate-peptide, and PET scans were obtained. Tumor was clearly visualized relative to background as early as 0.5 h after injection for both peptides (Fig. 3). As was the case for the ^{64}Cu-DOTA versions of the peptides (*13*), ^{18}F-fluorobenzoate-$R_0$1 exhibits greater tumor uptake (2.3 ± 0.6 %ID/g) than ^{18}F-fluorobenzoate-$S_0$2 (1.3% ± 0.4%), and both have comparable tumor-to-muscle ratios: 3.1 ± 1.0 and 2.9 ± 0.4 at 0.5 and 1 h, respectively, for ^{18}F-fluorobenzoate-$R_0$1, and 2.7 ± 0.4 and 4.0 ± 1.0 at 0.5 and 1 h, respectively, for ^{18}F-fluorobenzoate-$S_0$2 (Fig. 4).

To further demonstrate integrin $\alpha_v\beta_6$ specificity, small-animal PET experiments were performed with xenografted tumors of 293 cells, which do not express integrin $\alpha_v\beta_6$ (*13*). ^{18}F-fluorobenzoate-$R_0$1 exhibits 1.4 ± 0.6 %ID/g tumor signal, which is significantly less (P = 0.04) than BxPC3 xenografts (Figs. 3 and 4). Likewise, ^{18}F-fluorobenzoate-$S_0$2 has lower uptake in 293 tumors than in BxPC3 tumors (0.5% ± 0.2%, P = 0.02).

Both tracers exhibit modest kidney uptake (27% ± 4% for ^{18}F-fluorobenzoate-$R_0$1 and 18% ± 6% for ^{18}F-fluorobenzoate-$S_0$2) and low liver uptake (2.0% ± 0.7% for ^{18}F-fluorobenzoate-$R_0$1 and 0.9% ± 0.3% for ^{18}F-fluorobenzoate-$S_0$2) (Supplemental Fig. 2).

Dynamic PET demonstrates the rapid distribution of the peptides, because tumor targeting is 95% complete within 5 min for both peptides (Fig. 5). The rapid tumor signal stabilization is consistent with the rapid clearance of both peptides: analysis of the radioactivity in the heart reveals blood clearance half-times of 1.6 min for ^{18}F-fluorobenzoate-$R_0$1 and 1.8 min for ^{18}F-fluorobenzoate-$S_0$2 (Fig. 5). Rapid dynamics are observed in other tissues (Supplemental Fig. 3).

Tissue Biodistribution

Further tissue biodistribution was obtained via activity measurements of resected tissues from mice euthanized at 0.5 and 2 h after injection (Fig. 6). These data closely match the PET results for tumor, muscle, kidney, and liver. Tumor uptake is higher in target-positive (BxPC3) tumors than in target-negative (293) tumors at 0.5 h: 2.2 ± 0.5 vs. 0.6 ± 0.1 %ID/g for ^{18}F-fluorobenzoate-$R_0$1 (P = 0.027) and 0.71 ± 0.13 vs. 0.11 ± 0.02 %ID/g for ^{18}F-fluorobenzoate-$S_0$2 (P = 0.001). At 2 h, the uptake values are 1.4 ± 0.3 vs. 0.9 ± 0.6 %ID/g (^{18}F-fluorobenzoate-$R_0$1, P = 0.13) and 0.24 ± 0.06 vs. 0.10 ± 0.05 %ID/g (^{18}F-fluorobenzoate-$S_0$2, P = 0.006). Tumor-to-blood ratios of 6.0 ± 1.1 and 3.1 ± 0.8 were achieved at 2 h for ^{18}F-fluorobenzoate-$R_0$1 and ^{18}F-fluorobenzoate-$S_0$2, respectively. Low nontarget uptake is observed in other tissues aside from moderate uptake in the stomach (1.6% ± 0.4%, n = 8) and lungs (2.9% ± 1.2%, n = 8; though because of the low density of lungs, the uptake is only 0.7 ± 0.3 %ID/cm^3) for ^{18}F-fluorobenzoate-$R_0$1.

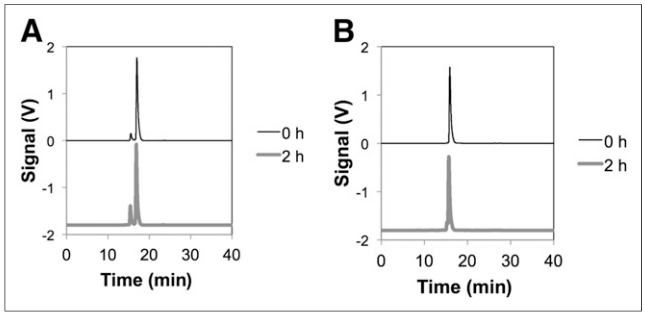

FIGURE 2. Serum stability. ^{18}F-fluorobenzoate-$R_0$1 (A) and ^{18}F-fluorobenzoate-$S_0$2 (B) were incubated in 50% human serum at 37°C for 2 h. Samples were separated by RP-HPLC on C18 column with gradient of 5%–85% acetonitrile in water (both with 0.1% trifluoroacetic acid) from 5 to 35 min and analyzed with a γ-ray detector.

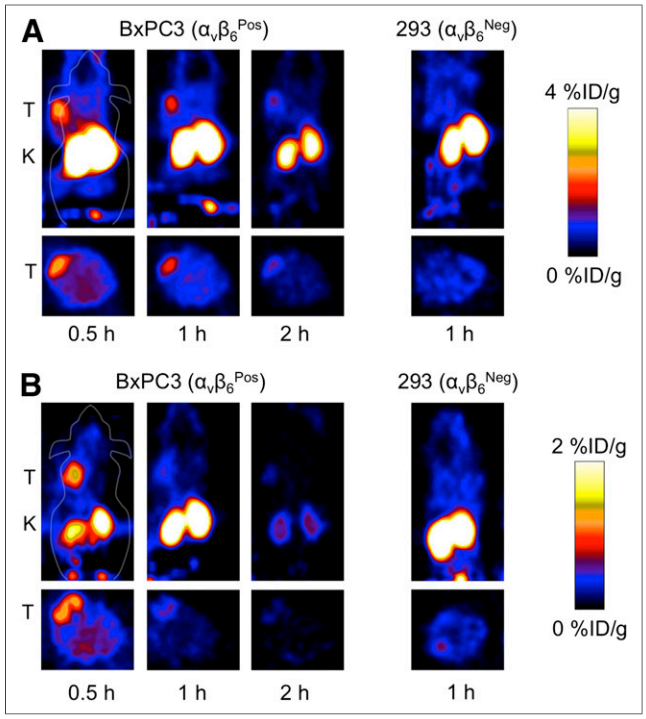

FIGURE 3. Small-animal PET imaging. BxPC3 pancreatic adenocarcinoma cells (integrin $\alpha_v\beta_6$–positive) or 293 (integrin $\alpha_v\beta_6$–negative) were xenografted into nude mice. ^{18}F-fluorobenzoate-$R_0$1 (2–3 MBq) (A) or ^{18}F-fluorobenzoate-$S_0$2 (2–3 MBq) (B) were injected via tail vein. Five-minute static scans were acquired at 0.5, 1, and 2 h after injection. Decay-corrected coronal and transverse slices are presented. Tumor (T) and kidneys (K) are marked on images. Images are all normalized to quantitative color scale shown on right of each figure set.

DISCUSSION

We previously validated the engineered $R_0$1 and $S_0$2 peptides as targeting domains for molecular PET imaging of integrin $\alpha_v\beta_6$ using ^{64}Cu (*13*). Radiolabeling these peptides with ^{18}F better matches radioisotope kinetics (1.8-h half-time), with the rapid uptake in tumor and clearance from background (effective imaging at 1 h after injection) for more efficient use of dose, which is critical for clinical translation. The peptides were effectively labeled site-specifically at the N-terminal amine with ^{18}F using SFB and retained high stability and activity. The tracers specifically

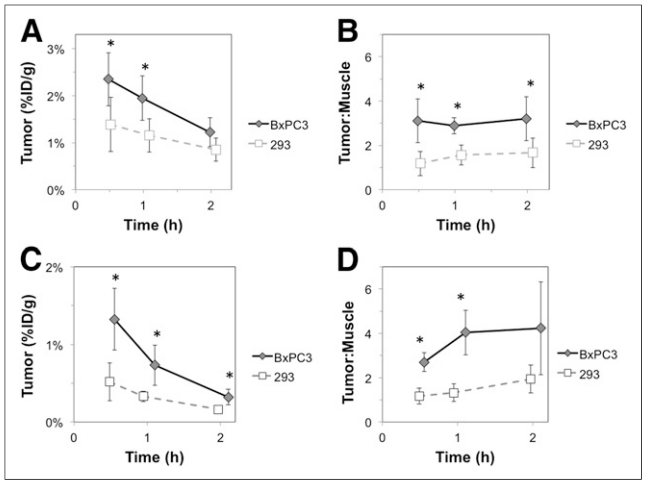

FIGURE 4. Small-animal PET quantification of data in Figure 3. Signals in tumor and muscle were quantified with AsiPro VM. Value and error bars represent mean and SD for ^{18}F-fluorobenzoate-$R_0$1 (A and B; $n = 5$ for BxPC3, $n = 3$ for 293) and ^{18}F-fluorobenzoate-$S_0$2 (C and D; $n = 4$ for BxPC3, $n = 4$ for 293). *$P < 0.05$.

target tumor (5.0 ± 1.8 and 4.7 ± 1.8 tumor to muscle and 6.0 ± 1.1 and 3.1 ± 0.8 tumor to blood for ^{18}F-fluorobenzoate-$R_0$1 and ^{18}F-fluorobenzoate-$S_0$2, respectively) in an integrin $\alpha_V\beta_6$–specific manner (statistically significantly reduced uptake in target-negative 293 xenografts).

We have also explored coinjection studies with unlabeled peptide. $R_0$1 coinjection decreases tumor uptake, albeit not to a statistically significant extent: 2.2 ± 0.5 %ID/g in BxPC3 tumors at 0.5 h versus 1.8 ± 0.4 %ID/g with cold peptide coinjection. $S_0$2 does not demonstrate tumor uptake reduction. The lack of impact is potentially due to blocking of dilute levels of nontumor integrin $\alpha_v\beta_6$, thereby freeing more peptide for tumor targeting (*20*). Although this avenue is under further investigation, the target-positive and target-negative tumor comparisons, via both PET and excised tissue analysis, demonstrate specificity.

In addition to improved positron yield and reduced dosimetry relative to ^{64}Cu, the ^{18}F versions of these peptides have greatly reduced liver and kidney uptake. $R_0$1 exhibits a 5-fold reduction in renal signal (in %ID/g) from 80 ± 16 for ^{64}Cu-DOTA to 16 ± 4 for ^{18}F-fluorobenzoate at 1 h. $S_0$2 decreases 4-fold from 29 ± 10 to 7 ± 3. Hepatic signal (in %ID/g) decreases from 3.1 ± 0.6 to 1.2 ± 0.2 for $R_0$1 and from 4.4 ± 1.2 to 0.3 ± 0.1 for $S_0$2. This

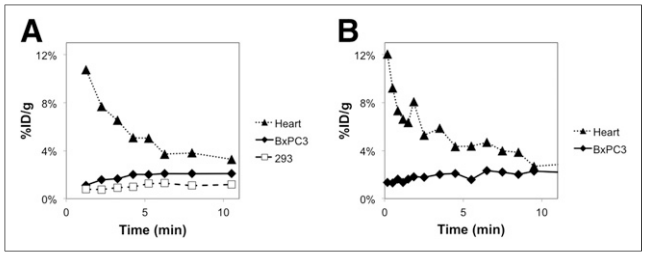

FIGURE 5. Dynamic PET. BxPC3 pancreatic adenocarcinoma cells (integrin $\alpha_v\beta_6$–positive) or 293 (integrin $\alpha_v\beta_6$–negative) were xenografted into nude mice. ^{18}F-fluorobenzoate-$R_0$1 (2–3 MBq) (A) or ^{18}F-fluorobenzoate-$S_0$2 (2–3 MBq) (B) were injected via tail vein. Ten-minute dynamic scan was acquired via PET. Mean signals in ellipsoid regions of interest were quantified with AMIDE.

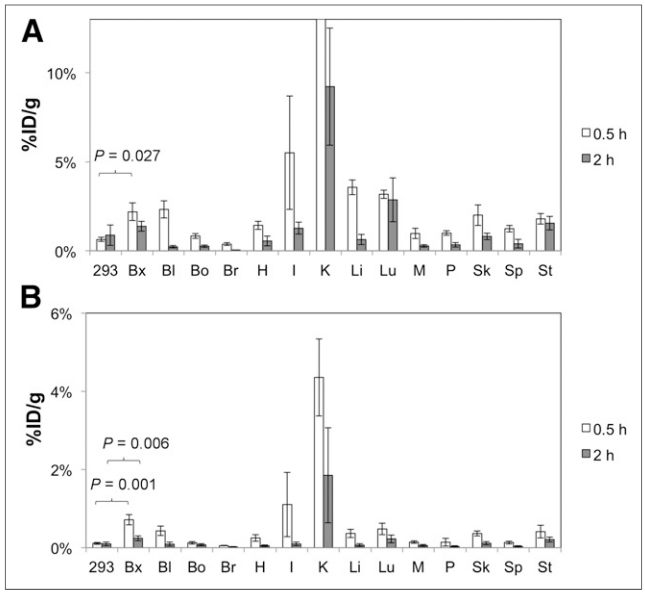

FIGURE 6. Biodistribution. BxPC3 pancreatic adenocarcinoma cells (integrin $\alpha_v\beta_6$–positive) or 293 (integrin $\alpha_v\beta_6$–negative) were xenografted into nude mice. ^{18}F-fluorobenzoate-$R_0$1 (2–3 MBq) (A; 0.5 h: $n = 3$ for BxPC3, $n = 3$ for 293, $n = 6$ for nontumor values; 2 h: $n = 5$ for BxPC3, $n = 3$ for 293, $n = 8$ for nontumor values) or ^{18}F-fluorobenzoate-$S_0$2 (2–3 MBq) (B; 0.5 h: $n = 3$ for BxPC3, $n = 3$ for 293, $n = 6$ for nontumor values; 2 h: $n = 4$ for BxPC3, $n = 4$ for 293, $n = 8$ for nontumor values) were injected via tail vein. Mice were euthanized at 0.5 or 2 h after injection. Tissues were collected, and decay-corrected activity relative to injected dose was determined per gram of tissue (%ID/g). Value and error bars represent mean and SD. Values are presented for *Bl* = blood; *Bo* = bone; *Br* = brain; Bx = BxPC3 tumor; *H* = heart; *I* = intestine; *K* = kidney; *Li* = liver; *Lu* = lungs; *M* = muscle; *P*= pancreas; *Sk* = skin; *Sp* = spleen; *St* = stomach.

renal reduction is in agreement with previously observed results for several Affibody domains. Affibody $Z_{HER2:477}$ kidney uptake (in %ID/g) was reduced from 206 ± 22 to 19 ± 1 for the monomer and from 114 ± 11 to 7 ± 1 for the dimer when labeling was changed from ^{64}Cu-DOTA (*21*) to ^{18}F-*N*-(4-fluorobenzylidene)oxime (*22*). Similarly, Affibody $Z_{HER2–342}$ kidney uptake (in %ID/g) decreased from 172 ± 13 at 4 h with ^{111}In-DOTA (*23*) to 10 ± 3 at 2 h with *N*-2-(4-^{18}F-fluorobenzamido)ethylmaleimide (*24*).

Tumor uptake is also reduced in the ^{18}F-labeled peptides relative to the ^{64}Cu-labeled peptides, although to a lesser extent than the beneficial kidney and liver reductions. $R_0$1 tumor signal (in %ID/g) decreases from 4.7 ± 0.9 at 1 h to 2.3 ± 0.6 and 1.9 ± 0.5 at 0.5 and 1 h, respectively. $S_0$2 decreases from 2.1 ± 0.5 at 1 h to 1.3 ± 0.4 and 0.7 ± 0.3 at 0.5 and 1 h, respectively. As noted above, molecular specificity remains high in relation to muscle, blood, and integrin $\alpha_V\beta_6$–negative tumors.

Thus, ^{18}F-fluorobenzoate-$R_0$1 is a prime candidate for clinical translation. Though only semiquantitative comparisons can be made because of the use of different animal models, ^{18}F-fluorobenzoate-$R_0$1 compares favorably to alternative integrin $\alpha_V\beta_6$ tracers. This probe has greater tumor uptake (2.3 ± 0.6 and 1.9 ± 0.5 at 0.5 and 1 h, respectively, for ^{18}F-fluorobenzoate-$R_0$1 vs. 0.7 ± 0.2 for ^{18}F-fluorobenzoate-A20FMDV2 at 1 h), tumor-to-muscle contrast (5.0 ± 1.8 vs. 1.3), and tumor-to-blood contrast (6.0 ± 1.1 vs. 3.3) than ^{18}F-A20FMDV2, albeit with higher renal signal (27 ± 4 and 16 ± 4 at 0.5 h and 1 h, respectively,

vs. 3.3 ± 0.8). The addition of polyethylene glycol to the A20FMDV2 peptide (*11*) increased the tumor (1.9 ± 0.4) and kidney (19 ± 5) to uptake values essentially equal to those observed for ^{18}F-fluorobenzoate-$R_0$1. Importantly, ^{18}F-fluorobenzoate-$R_0$1 is 87% stable in human serum for 2 h whereas urine analysis at 1 h after injection reveals 3 metabolites and no intact tracer for ^{18}F-A20 and 1 major metabolite for ^{18}F-PEG-A20FMDV2 (though data were not shown). Increased stability, a hallmark of the cystine knot scaffold (*25*), may reduce off-target effects from metabolites including reduced immunogenicity, which is now under study.

A clinical molecular imaging agent for integrin $\alpha_V\beta_6$ could have broad impact because increased expression is observed on multiple cancers (*1–9*). In particular, because of the metastatic potential and lethality of pancreatic cancer, there is a critical need for a molecular imaging agent for patient staging, treatment stratification, and therapy monitoring. Integrin $\alpha_V\beta_6$ expression is undetectable in healthy pancreas but has elevated expression in pancreatic ductal adenocarcinoma (*2*). It is noteworthy that the PET tracers in the current work exhibit low uptake in healthy pancreas (0.3% ± 0.1% for ^{18}F-fluorobenzoate-$R_0$1 and 0.03% ± 0.01% for ^{18}F-fluorobenzoate-$S_0$2), which is imperative for clinical translation toward this application.

CONCLUSION

These cystine knot peptide tracers, in particular ^{18}F-fluorobenzoate-$R_0$1, show translational promise for molecular imaging of integrin $\alpha_v\beta_6$ overexpression in pancreatic and other cancers.

DISCLOSURE

The costs of publication of this article were defrayed in part by the payment of page charges. Therefore, and solely to indicate this fact, this article is hereby marked "advertisement" in accordance with 18 USC section 1734. This research was supported by the National Institutes of Health (grants CA119367, CA136465, CA083636, and CA114747), the Department of Energy (Stanford Molecular Imaging Research and Training Program), the Canary Foundation, and a postdoctoral fellowship from the American Cancer Society. No other potential conflict of interest relevant to this article was reported.

REFERENCES

1. Breuss JM, Gallo J, DeLisser HM, et al. Expression of the beta 6 integrin subunit in development, neoplasia and tissue repair suggests a role in epithelial remodeling. *J Cell Sci.* 1995;108:2241–2251.
2. Sipos B, Hahn D, Carceller A, et al. Immunohistochemical screening for beta6-integrin subunit expression in adenocarcinomas using a novel monoclonal antibody reveals strong up-regulation in pancreatic ductal adenocarcinomas in vivo and in vitro. *Histopathology.* 2004;45:226–236.
3. Maubant S, Cruet-Hennequart S, Dutoit S, et al. Expression of alpha V-associated integrin beta subunits in epithelial ovarian cancer and its relation to prognosis in patients treated with platinum-based regimens. *J Mol Histol.* 2005;36:119–129.
4. Orimoto AM, Neto CF, Pimentel ERA, et al. High numbers of human skin cancers express MMP2 and several integrin genes. *J Cutan Pathol.* 2008;35:285–291.
5. Bates RC, Bellovin DI, Brown C, et al. Transcriptional activation of integrin beta6 during the epithelial-mesenchymal transition defines a novel prognostic indicator of aggressive colon carcinoma. *J Clin Invest.* 2005;115:339–347.
6. Elayadi AN, Samli KN, Prudkin L, et al. A peptide selected by biopanning identifies the integrin $\alpha_v\beta_6$ as a prognostic biomarker for nonsmall cell lung cancer. *Cancer Res.* 2007;67:5889–5895.
7. Hazelbag S, Kenter GG, Gorter A, et al. Overexpression of the alpha v beta 6 integrin in cervical squamous cell carcinoma is a prognostic factor for decreased survival. *J Pathol.* 2007;212:316–324.
8. Zhang Z-Y, Xu K-S, Wang J-S, et al. Integrin alphanvbeta6 acts as a prognostic indicator in gastric carcinoma. *Clin Oncol (R Coll Radiol).* 2008;20:61–66.
9. Yang G-Y, Xu K-S, Pan Z-Q, et al. Integrin alpha v beta 6 mediates the potential for colon cancer cells to colonize in and metastasize to the liver. *Cancer Sci.* 2008;99:879–887.
10. Hausner SH, DiCara D, Marik J, Marshall JF, Sutcliffe JL. Use of a peptide derived from foot-and-mouth disease virus for the noninvasive imaging of human cancer: generation and evaluation of 4-[^{18}F]fluorobenzoyl A20FMDV2 for in vivo imaging of integrin $\alpha_v\beta_6$ expression with positron emission tomography. *Cancer Res.* 2007;67:7833–7840.
11. Hausner SH, Abbey CK, Bold RJ, et al. Targeted in vivo imaging of integrin $\alpha_v\beta_6$ with an improved radiotracer and its relevance in a pancreatic tumor model. *Cancer Res.* 2009;69:5843–5850.
12. Nothelfer E-M, Zitzmann-Kolbe S, Garcia-Boy R, et al. Identification and characterization of a peptide with affinity to head and neck cancer. *J Nucl Med.* 2009;50:426–434.
13. Kimura RH, Teed R, Hackel BJ, et al. Pharmacokinetically stabilized cystine knot peptides that bind alpha-v-beta-6 integrin with single-digit nanomolar affinities for detection of pancreatic cancer. *Clin Cancer Res.* 2012;18:839–849.
14. Howlader N, Noone A, Krapcho M, et al. *SEER Cancer Statistics Review, 1975–2008.* Bethesda, MD: National Cancer Institute; 2011.
15. Chen X, Park R, Shahinian AH, et al. ^{18}F-labeled RGD peptide: initial evaluation for imaging brain tumor angiogenesis. *Nucl Med Biol.* 2004;31:179–189.
16. Cai W, Olafsen T, Zhang X, et al. PET imaging of colorectal cancer in xenograft-bearing mice by use of an ^{18}F-labeled T84.66 anti-carcinoembryonic antigen diabody. *J Nucl Med.* 2007;48:304–310.
17. Lipovsek D, Lippow SM, Hackel BJ, et al. Evolution of an interloop disulfide bond in high-affinity antibody mimics based on fibronectin type III domain and selected by yeast surface display: molecular convergence with single-domain camelid and shark antibodies. *J Mol Biol.* 2007;368:1024–1041.
18. Cheng Y, Prusoff WH. Relationship between the inhibition constant (K1) and the concentration of inhibitor which causes 50 per cent inhibition (I50) of an enzymatic reaction. *Biochem Pharmacol.* 1973;22:3099–3108.
19. Loening AM, Gambhir SS. AMIDE: a free software tool for multimodality medical image analysis. *Mol Imaging.* 2003;2:131–137.
20. Miao Z, Ren G, Liu H, Jiang L, Cheng Z. Small-animal PET imaging of human epidermal growth factor receptor positive tumor with a ^{64}Cu labeled affibody protein. *Bioconjug Chem.* 2010;21:947–954.
21. Cheng Z, Jesus OP, Kramer DJ, et al. ^{64}Cu-Labeled affibody molecules for imaging of HER2 expressing tumors. *Mol Imaging Biol.* 2010;12:316–324.
22. Cheng Z, De Jesus OP, Namavari M, et al. Small-animal PET imaging of human epidermal growth factor receptor type 2 expression with site-specific ^{18}F-labeled protein scaffold molecules. *J Nucl Med.* 2008;49:804–813.
23. Ahlgren S, Orlova A, Rosik D, et al. Evaluation of maleimide derivative of DOTA for site-specific labeling of recombinant affibody molecules. *Bioconjug Chem.* 2008;19:235–243.
24. Kramer-Marek G, Kiesewetter DO, Capala J. Changes in HER2 expression in breast cancer xenografts after therapy can be quantified using PET and ^{18}F-labeled affibody molecules. *J Nucl Med.* 2009;50:1131–1139.
25. Moore SJ, Leung CL, Cochran JR. Knottins: disulfide-bonded therapeutic and diagnostic peptides. *Drug Discov Today Technol.* 2012;9:e3–e11.

JNM The Journal of NUCLEAR MEDICINE

^{18}F-Fluorobenzoate–Labeled Cystine Knot Peptides for PET Imaging of Integrin $\alpha_v\beta_6$

Benjamin J. Hackel, Richard H. Kimura, Zheng Miao, Hongguang Liu, Ataya Sathirachinda, Zhen Cheng, Frederick T. Chin and Sanjiv S. Gambhir

J Nucl Med. 2013;54:1101-1105.
Published online: May 13, 2013.
Doi: 10.2967/jnumed.112.110759

The Journal of Nuclear Medicine is published monthly.
SNMMI | Society of Nuclear Medicine and Molecular Imaging
1850 Samuel Morse Drive, Reston, VA 20190.
(Print ISSN: 0161-5505, Online ISSN: 2159-662X)

SNMMI SOCIETY OF NUCLEAR MEDICINE AND MOLECULAR IMAGING